

# Cobalt-substitution-induced Superconductivity in a New Compound with ZrCuSiAs-type Structure, SrFeAsF

Satoru Matsuishi<sup>1</sup>, Yasunori Inoue<sup>2</sup>, Takatoshi Nomura<sup>2</sup>, Masahiro Hirano<sup>1,3</sup> and Hideo Hosono<sup>1,2,3</sup>

<sup>1</sup>*Frontier Research Center, Tokyo Institute of Technology, Mail Box S2-13, 4259 Nagatsuta, Midori-ku, Yokohama 226-8503, Japan*

<sup>2</sup>*Materials and Structures Laboratory, Tokyo Institute of Technology, Mail Box R3-1, 4259 Nagatsuta, Midori-ku, Yokohama 226-8503, Japan*

<sup>3</sup>*ERATO-SORST, JST, Frontier Research Center, Tokyo Institute of Technology, Mail Box S2-13, 4259 Nagatsuta, Midori-ku, Yokohama 226-8503, Japan.*

(Received XXX X, 2008)

We have synthesized a quaternary fluoroarsenide SrFeAsF with the ZrCuSiAs-type structure (P4/nmm,  $a = 0.3999$  and  $c = 0.8973$  nm), which is composed of an alternately stacked  $(\text{FeAs})^{\delta^-}$  and  $(\text{SrF})^{\delta^+}$  layers, analogous to the FeAs-based superconductor LaFeAsO. SrFeAsF shows metallic type conduction with the anomaly at  $\sim 180$  K. The partial replacement of the Fe with Co suppresses the anomaly and induces the superconductivity, while the maximal  $T_c$  (4 K for  $\text{SrFe}_{0.875}\text{Co}_{0.125}\text{AsF}$ ) is much lower than that of the Co-substituted LaFeAsO. Replacement of  $(\text{LaO})^{\delta^+}$  layers with  $(\text{SrF})^{\delta^+}$  layers results in a enlargement of the  $c$ -axis length (+2.6%). These results suggest the importance of interlayer interaction as a critical  $T_c$ -controlling factor in FeAs-based superconductors.

KEYWORDS: superconductivity, iron-based superconductor, ZrCuSiAs-type structure

The discovery of superconductivity in F-doped LaFeAsO with  $T_c = 26$  K<sup>1)</sup> triggered intensive studies of FeAs-based layered compound systems including  $R$ FeAsO ( $R$  = rare-earth) and  $A$ Fe<sub>2</sub>As<sub>2</sub> ( $A$  = alkali-earth) with a hope to realizing further high- $T_c$  superconductors.<sup>2-11)</sup> These efforts lead to raising  $T_c$  up to 56 K in Th-doped GdFeAsO so far.<sup>8)</sup> The parent compounds for these superconductors belong to the ZrCuSiAs-type structure (space group P4/nmm) or ThCr<sub>2</sub>Si-type structure (space group I4/mmm), consisting of an alternating stack of (FeAs) <sup>$\delta^-$</sup>  and (RO) <sup>$\delta^+$</sup>  or  $A$  <sup>$\delta^+$</sup>  layers. They suffer a crystallographic transition from the tetragonal to orthogonal, accompanying with antiferromagnetic spin ordering at 140-200 K.<sup>1,3,8-14)</sup> Electron or hole doping to the (FeAs) <sup>$\delta^-$</sup>  layer through the doping of F<sup>-</sup> ions at the O sites of insulating layers in RFeAsO, for instance, (modulation doping) suppressed both transitions, resulting in emergence of the superconducting phase. Thus, the presence of the magnetic and/or charge instabilities is considered to be a key factor for the high- $T_c$ . The efforts in the material studies have been focused on the synthesis of ZrCuSiAs-type and related-type compounds containing the square iron lattice<sup>15-19)</sup> as well as on the carrier doping technique. Three successful doping methods have been reported to date, i.e., electron-doping by the oxygen-vacancy formation in insulating layers (RO) <sup>$\delta^+$</sup>  in RFeAsO,<sup>20,21)</sup> hole-doping by alkali-metal doping to  $A$  <sup>$\delta^+$</sup>  layer in AFe<sub>2</sub>As<sub>2</sub><sup>9-11)</sup> and electron-doping by partial replacement of Fe with Co in RFeAsO and AFe<sub>2</sub>As<sub>2</sub>.<sup>22-26)</sup> Effectiveness of the last technique in FeAs-based system is quite unique in comparison with high temperature cuprates.<sup>27)</sup>

Here, we report the synthesis of a new FeAs containing ZrCuSiAs-type compound, SrFeAsF, in which the (FeAs) <sup>$\delta^-$</sup>  layer is sandwiched by (SrF) <sup>$\delta^+$</sup>  layer (inset of Fig 1a) and emergence of superconductivity by electron-doping to this material utilizing a partial substitution of Fe<sup>2+</sup> ions with a 3d<sup>6</sup> electronic configuration with Co<sup>2+</sup> ions with a 3d<sup>7</sup>. It is noted that  $T_c = 4$  K is realized for the Co content of 12.5 % (SrFe<sub>0.875</sub>Co<sub>0.125</sub>AsF), which is much lower than  $T_c$  in Co-substituted FeAs-based compound ( $T_c = 14$  K for LaFeAsO, 17 K for SmFeAsO, 20 K for SrFe<sub>2</sub>As<sub>2</sub>, and 22 K for BaFe<sub>2</sub>As<sub>2</sub>).<sup>22-26)</sup> These findings suggest, (1)  $T_c$  value is sensitive to the blocking layer, although FeAs layer seems to be essential for the high  $T_c$  superconductivity, providing new information for governing factors for the  $T_c$  values. (2) More generally, high  $T_c$  superconductors still remain in a large number of ZrCuSiAs and related type crystals.<sup>28)</sup>

Samples were prepared by a solid state reaction of SrF<sub>2</sub> (99.99 %), SrAs, Fe<sub>2</sub>As and Co<sub>2</sub>As: SrF<sub>2</sub> + SrAs + (1-x) Fe<sub>2</sub>As + x Co<sub>2</sub>As → 2SrFe<sub>1-x</sub>Co<sub>x</sub>AsF. SrAs was synthesized by heating a mixture of Sr shots (99.99 wt. %) and As powders (99.9999 wt. %) at 650°C for 10 h in an evacuated silica tube. Fe<sub>2</sub>As and Co<sub>2</sub>As were synthesized from powders of respective elements at 800 °C for 10 h (Fe: 99.9 wt. %; Co: 99 wt. %). These products were then mixed in stoichiometric ratios, pressed, and heated in evacuated silica tubes at 1000 °C for 10 h to obtain sintered pellets. All the starting material preparation procedures were carried out in an Ar-filled glove box (O<sub>2</sub>, H<sub>2</sub>O < 1 ppm).

The crystal structure and lattice constants of the materials were examined by powder X-ray diffraction (XRD; Bruker D8 Advance TXS) using Cu K $\alpha$  radiation from a rotating anode with an aid of Rietveld refinement using Code TOPAS3.<sup>29)</sup> Temperature dependence of DC electrical resistivity ( $\rho$ ) at 2-300 K was measured by a four-probe technique using platinum electrodes deposited on samples. Magnetization ( $M$ ) measurements were performed with a vibrating sample magnetometer (Quantum Design) in the same temperature range.

Figure 1 shows powder XRD patterns of undoped (a) and 12.5 atom% Co-substituted SrFeAsF (b). Almost all the peaks are assigned to those of the SrFeAsF phase, except several weak peaks arising from impurity phases (SrF<sub>2</sub> and FeAs, the volume fraction of these impurity phases being 3 % at most). The SrFeAsF phase is tetragonal symmetry with room-temperature lattice constants of  $a$  = 0.3999 nm and  $c$  = 0.8973 nm for the undoped sample and  $a$  = 0.4002 nm and  $c$  = 0.8943 nm for the 12.5 atom% Co-substituted sample (See Table I). The  $c$ -axis length of SrFeAsF is larger by 2.6 % than that of LaFeAsO, while  $a$  -axis length is smaller by 0.8 %.<sup>12)</sup> In contrast to the replacement of La with other rare-earth ion (Ce, Pr, Nd, and Sm), the replacement of (LaO) <sup>$\delta+$</sup>  layer with (SrF) <sup>$\delta+$</sup>  layer leads to the shrinkage of  $a$ -axis length and the expansion of  $c$ -axis length. Upon substituting the Fe sites with Co, the  $c$ -axis length monotonically decreases with nominal Co concentration below 20 %, while the  $a$ -axis length remains almost constant (Fig.1b). The decrease in the  $c$ -axis indicates the enhanced Coulombic interaction between the (SrF) <sup>$\delta+$</sup>  and (FeAs) <sup>$\delta-$</sup>  layers with the Co content, providing evidence that the Co-substitution adds excess electrons to the (FeAs) <sup>$\delta-$</sup>  layers.

Figure 2 (a) shows temperature ( $T$ ) dependences of  $\rho$  and molar magnetic susceptibility ( $\chi_{\text{mol}}$ ) for undoped SrFeAsF. The  $\chi_{\text{mol}}-T$  curve was obtained under the magnetic field ( $H$ ) of 1 T with a zero field cooling mode. With a decrease in temperature, both  $\rho-T$  and  $\chi_{\text{mol}}-T$  curves exhibit sudden decreases at  $\sim 180$  K ( $T_{\text{anom}}$ ). This behavior is quite analogous to those of  $R\text{FeAsO}$  and  $A\text{Fe}_2\text{As}_2$ , indicating that the crystallographic transition accompanying with the magnetic order also occurs in SrFeAsF. As shown in Figure 2(b), 12.5% Co-doping apparently suppresses the anomaly, inducing superconductivity with the onset transition temperature ( $T_{\text{onset}}$ ) of 4.8 K (See inset).  $T_c$  defined as temperature where the  $\rho$  value becomes half of that at  $T_{\text{onset}}$  is 4 K. The sudden decrease in  $\chi_{\text{mol}}$  due to the diamagnetism induced by the superconducting transition is also observed below  $T_c$ . Figure 2(c) shows volume magnetic susceptibility ( $4\pi\chi$ ) vs.  $T$  plots under zero-field cooling (ZFC) and field cooling (FC) with  $H = 1$  mT. For small magnetic field ( $< 1$  mT), diamagnetic signal due to superconductivity is much larger than the paramagnetic signal, while it is masked by paramagnetic component in the high magnetic field region. Figure 2(d) shows the  $M-H$  plot for  $\text{SrFe}_{0.875}\text{Co}_{0.125}\text{AsF}$  at 2 K, which demonstrate diamagnetic shielding below 1 mT. The volume fraction of the superconducting phase estimated from the slope of  $M-H$  curve in the region of 0-0.2 mT is  $\sim 17$  %.

Figure 3(a) shows  $\rho-T$  curves for Co-substituted SrFeAsF samples with several  $x$  values. For  $x = 0.05$  and 0.075, the anomaly, observed in sample with  $x = 0$  at  $\sim 180$  K, still appears as a small dull peak and the peak temperature shifts to lower temperatures with an increase in  $x$ . For  $x = 0.1$  and 0.125, the anomaly is completely suppressed and the superconducting transition is observed ( $T_{\text{onset}} \sim 2$  K for  $x = 0.1$ ). Further increase in the Co concentration above 15 % breaks the superconductivity and metallic conductivity ( $d\rho/dT > 0$ ) is observed above  $T_{\text{min}}$ . The minimum ( $T_{\text{min}}$ ) is observed to exist in the  $\rho-T$  curves in the tetragonal phase for all Co concentrations. Figure 3(b) summarizes  $T_{\text{anom}}$ ,  $T_{\text{onset}}$  and  $T_{\text{min}}$  as a function of  $x$ , demonstrating the Co-doping induces the superconducting phase in SrFeAsF and the highest  $T_c$  of 4 K is attained at  $x = 0.125$ .

Last, the present results are compared with those reported for other FeAs-based superconductors. It is worth noting that the threshold and optimal electron-doping levels

are close to those of Co-substituted LaFeAsO and SmFeAsO although the  $T_c$  value is fairly smaller. Lee et al. proposed an idea on the basis of many data reported to date that  $T_c$  increases with the distortion of the FeAs<sub>4</sub> tetrahedra from the regular shape along the *c*-axis direction.<sup>28)</sup> However, the angles in SrFeAsF ( $\alpha = 111.1^\circ$ ) do not differ so largely from those of *R*FeAsO compounds (For example,  $\alpha = 110.8^\circ$  for SmFeAsO,  $\alpha = 113.3^\circ$  for LaFeAsO where  $\alpha = 109.5^\circ$  for regular tetrahedron),<sup>14</sup> indicating the distortion is not a dominant factor for the low  $T_c$  in the Co-substituted SrFeAsF. The most prominent structural change observed by the replacement of (LaO) <sup>$\delta+$</sup>  layers with (SrF) <sup>$\delta+$</sup>  layers is a large anisotropic change in the *a*- and *c*-axes (*a*-axis: -0.8%, *c*-axis: +2.6%), in particular enlargement of the *c*-axis length. To date, no importance of the *c*-axis length, has been pointed out along with an experimental finding in the Fe-based layered superconductors.

In summary, the electrical conductivity and magnetization measurements demonstrate Co-substituted SrFeAsF is a bulk superconductor.  $T_c$  changes with the Co-content, exhibiting the maximum of 4 K at the Co-content of ~12.5 atom %. Although the general feature of the phase diagram is similar to that of Co-substituted LaFeAsO in terms of the variation in  $T_c$ , and  $T_{\text{anom}}$  with the Co content,  $T_c$  is lowered significantly from LaO to SrF compounds. Crystallographic change in the FeAs layer cannot explain the large difference in  $T_c$ . These results suggest that expansion of the *c*-axis length yields a negative effect on  $T_c$ .

### Acknowledgment

We thank Drs. Sung Wng Kim, Takashi Mine, Hiroshi Yanagi and Youichi Kamihara for their helpful discussions.

- 1) Y. Kamihara, T. Watanabe, M. Hirano, H. Hosono: *J. Am. Chem. Soc.* **130** (2008) 3296.
- 2) H. Takahashi, K. Igawa, K. Arii, Y. Kamihara, M. Hirano, H. Hosono: *Nature* **453** (2008) 376.
- 3) G. F. Chen, Z. Li, D. Wu, G. Li, W. Z. Hu, J. Dong, P. Zheng, J. L. Luo, N. L. Wang: *Phys. Rev. Lett.* **100** (2008) 247002.
- 4) Z-A. Ren, J. Yang, W. Lu, W. Yi, G-C. Che, X-L. Dong, L-L. Sun, Z-X. Zhao: *Materials Research Innovations* **12** (2008) 105.
- 5) Z-A. Ren, J. Yang, W. Lu, W. Yi, Z-L. Shen, Z-C. Li, G-C. Che, X-L. Dong, L-L. Sun, F. Zhou, Z-X. Zhao: *Europhys. Lett.* **82** (2008) 57002.
- 6) X. H. Chen, T. Wu, G. Wu, R. H. Liu, H. Chen, D. F. Fang, *Nature* **453** (2008) 761.
- 7) Z-A. Ren, W. Lu, J. Yang, W. Yi, X-L. Shen, Z-C. Li, G-C. Che, X-L. Dong; L-L. Sun, F. Zhou, Z-X. Zhao: *Chin. Phys. Lett.*, **25** (2008) 2215.
- 8) C. Wang, L. Li, S. Chi, Z. Zhu, Z. Ren, Y. Li, Y. Wang, X. Lin, Y. Luo, S. Jiang, X. Xu, G. Cao, Z. Xu: *Europhy. Lett.* **83** (2008) 67006.
- 9) M. Rotter, M. Tegel, D. Johrendt: *Phys. Rev. Lett.* **101** (2008) 107006.
- 10) G. F. Chen, Z. Li, G. Li, W. Z. Hu, J. Dong, X. D. Zhang, P. Zheng, N. L. Wang, J. L. Luo: *Chin. Phys. Lett.* **25** (2008) 3403.
- 11) G. Wu, H. Chen, T. Wu, Y. L. Xie, Y. J. Yan, R. H. Liu, X. F. Wang, J. J. Ying, X. H. Chen: [cond-mat/0806.4279](#).
- 12) C. de la Cruz, Q. Huang, J. W. Lynn, J. Li, W. Ratcliff II, J. L. Zarestky, H. A. Mook, G. F. Chen, J. L. Luo, N. L. Wang, P. Dai: *Nature* **453** (2008) 899.
- 13) T. Nomura, S. W. Kim, Y. Kamihara, M. Hirano, P. V. Sushko, K. Kato, M. Takata, A. L. Shluger, H. Hosono: [cond-mat/0804.3569](#).
- 14) A. Martinelli, A. Palenzona, C. Ferdeghini, M. Putti, E. Emerich: [cond-mat/0808.1024](#).
- 15) X. C. Wang, Q. Q. Liu, Y. X. Lv, W. B. Gao, L. X. Yang, R. C. Yu, F. Y. Li, C. Q. Jin: [cond-mat/0806.4688](#).
- 16) F-C. Hsu, J-Y. Luo, K-W. Yeh, T-K. Chen, T-W. Huang, P. M. Wu, Y-C. Lee, Y-L. Huang, Y-Y. Chu, D-C. Yan, M-K. Wu: [cond-mat/0807.2369](#).
- 17) Y. Mizuguchi, F. Tomioka, S. Tsuda, T. Yamaguchi, Y. Takano: [cond-mat/0807.4315](#).
- 18) K-W. Yeh, T-W. Huang, Y-L. Huang, T-K. Chen, F-C. Hsu, P. M. Wu, Y-C. Lee, Y-Y.

- Chu, C-L. Chen, J-Y. Luo, D-C. Yan, M-K. Wu: cond-mat/0808.0474.
- 19) H. Hosono: J. Phys. Soc. Jpn. submitted
- 20) Z. A. Ren, G. C. Che, X. L. Dong, J. Yang, W. Lu, W. Yi, X. L. Shen, Z. C. Li, L. L. Sun, F. Zhou, and Z. X. Zhao: Europhys. Lett. **83** (2008) 17002.
- 21) H. Kito, H. Eisaki, and A. Iyo: J. Phys. Soc. Jpn. **77** (2008) 063707.
- 22) A. S. Sefat, A. Huq, M. A. McGuire, R. Jin, B. C. Sales, D. Mandrus: Phys. Rev. B **78** (2008) 104505.
- 23) G. Cao, C. Wang, Z. Zhu, S. Jiang, Y. Luo, S. Chi, Z. Ren, Q. Tao, Y. Wang, Z. Xu: cond-mat/0807.1304.
- 24) Y. K. Li, X. Lin, Z. W. Zhu, H. Chen, C. Wang, L. J. Li, Y. K. Luo, M. He, Q. Tao, H. Y. Li, G. H. Cao, Z. A. Xu: cond-mat/0808.3254.
- 25) A. S. Sefat, R. Jin, M. A. McGuire, B. C. Sales, D. J. Singh, D. Mandrus: Phys. Rev. Lett. **101** (2008) 117004.
- 26) A. Leithe-Jasper, W. Schnelle, C. Geibel, H. Rosner: cond-mat/0807.2223.
- 27) J. M. Tarascon, L. H. Greene, P. Barboux, W. R. McKinnon, G. W. Hull: Phys. Rev. B. **36** (1987) 8393.
- 28) R. Pottgen, D. Johrendt: cond-mat/0807.2138.
- 29) TOPAS, Version 3; Bruker AXS: Karlsruhe Germany, (2005).
- 28) C. H. Lee, A. Iyo, H. Eisaki, H. Kito, M. T. Fernandez-Diaz, T. Ito, K. Kihou, H. Matsuhata, M. Braden, K. Yamada: J. Phys. Soc. Jpn. **77** (2008), 083704.

Figure 1 (a) Powder XRD patterns of SrFeAsF (+) and Rietveld fit (red line): Green line is difference between these patterns. Bars at bottom show calculated Bragg diffraction positions of SrFeAsF and SrF<sub>2</sub>. Inset shows structure model of SrFeAsF. (b) XRD pattern of SrFe<sub>0.875</sub>Co<sub>0.125</sub>AsF. Inset shows lattice constants *a* and *b* as a function of Co content. Bars at bottom show calculated diffraction positions of SrFe<sub>0.875</sub>Co<sub>0.125</sub>AsF, SrF<sub>2</sub> and FeAs.

Figure 2 Electrical resistivity ( $\rho$ ) and molar magnetic susceptibility ( $\chi_{\text{mol}}$ ) vs. temperature ( $T$ ) plots for undoped SrFeAsF (a) and SrFe<sub>0.875</sub>Co<sub>0.125</sub>AsF (b).  $H = 1$  T for  $\chi_{\text{mol}}-T$  measurements. (c) Zero-field cooling (ZFC) and field cooling (FC) volume magnetic susceptibility ( $4\pi\chi$ ) vs.  $T$  plots for SrFe<sub>0.875</sub>Co<sub>0.125</sub>AsF with  $H = 1$  mT. (d) Magnetization ( $M$ ) vs. Magnetic Field ( $H$ ) plot for SrFe<sub>0.875</sub>Co<sub>0.125</sub>AsF. Volume fraction of superconducting phase is estimated from the slope of liner region of  $M-H$  curve (dashed line).

Figure 3 (a) Electrical resistivity versus temperature plot for SrFe<sub>1-x</sub>Co<sub>x</sub>AsF:  $x = 0.0, 0.05, 0.075, 0.10, 0.125, 0.15$  and  $0.2$ . Horizontal line under each plot denotes  $\rho / \rho_{300} = 0$  line. (b)  $T_c$ ,  $T_{\text{onset}}$  and  $T_{\text{min}}$  in the  $\rho-T$  curves as a function of  $x$ .  $T_c$  is defined as the temperature where the value becomes half of that at  $T_{\text{onset}}$ .  $T_{\text{anom}}$  values for  $x = 0, 0.05$  and  $0.75$  are also shown.

Table I. Atomic parameters of SrFeAsF and SrFe<sub>0.875</sub>Co<sub>0.125</sub>AsF (space group P4/nmm) determined by Rietveld refinements of powder X-ray diffraction data at 300 K.  $B_{eq}$  is the isotropic atomic displacement parameter.

<hr/> <hr/>						
(a) SrFeAsF						
$a = 3.999383(28)$ Å, $c = 8.97274(10)$ Å						
Atom	site	occ.	$x$	$y$	$z$	$B_{eq}$ (Å <sup>2</sup> )
Sr	2c	1	1/4	1/4	0.15903(13)	0.487(33)
Fe	2b	1	3/4	1/4	1/2	0.191(36)
As	2c	1	1/4	1/4	0.65280(18)	0.166(35)
F	2a	1	3/4	1/4	0	0.55(12)

<hr/> <hr/>						
(b) SrFe <sub>0.875</sub> Co <sub>0.125</sub> AsF						
$a = 4.001816(23)$ Å, $c = 8.943446(76)$ Å						
Atom	site	occ.	$x$	$y$	$z$	$B_{eq}$ (Å <sup>2</sup> )
Sr	2c	1	1/4	1/4	0.15821(12)	0.383(40)
Fe	2b	7/8	3/4	1/4	1/2	0.243(39)
Co	2b	1/8	3/4	1/4	1/2	0.243(39)
As	2c	1	1/4	1/4	0.65095(17)	0.130(40)
F	2a	1	3/4	1/4	0	0.72(13)

---



---

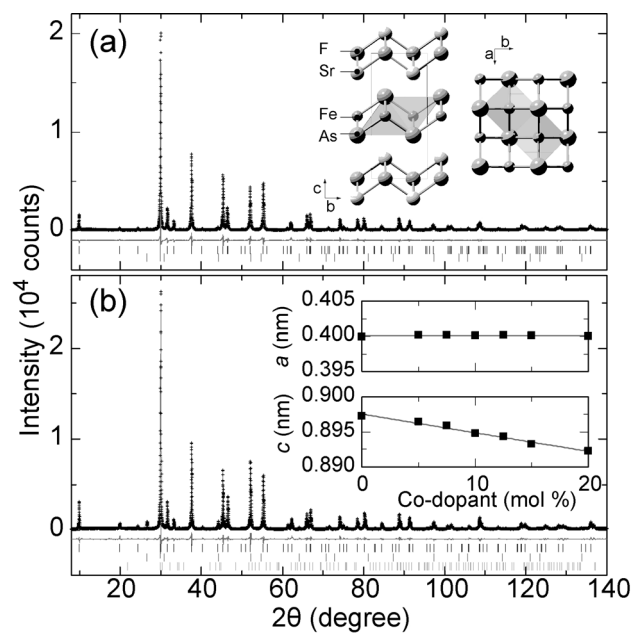


Fig.1

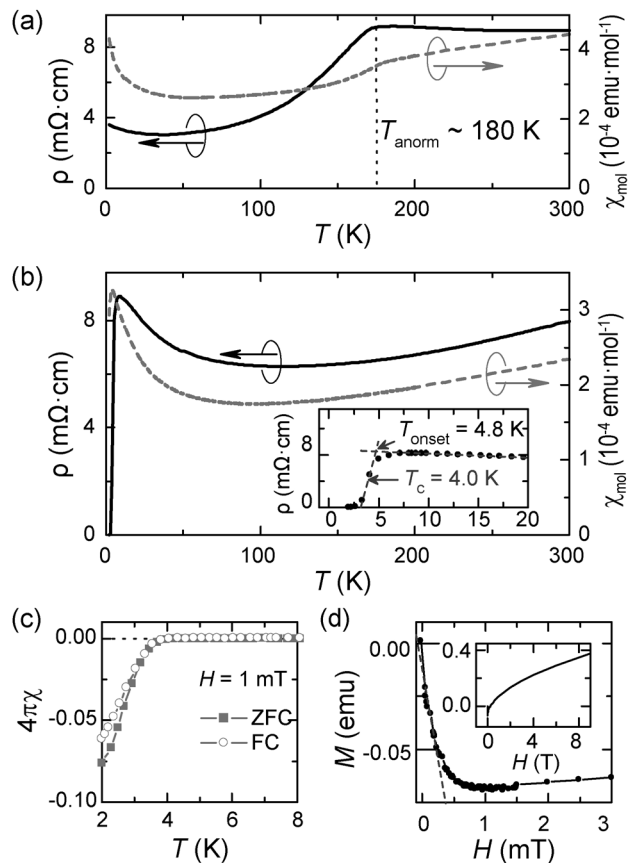


Fig. 2

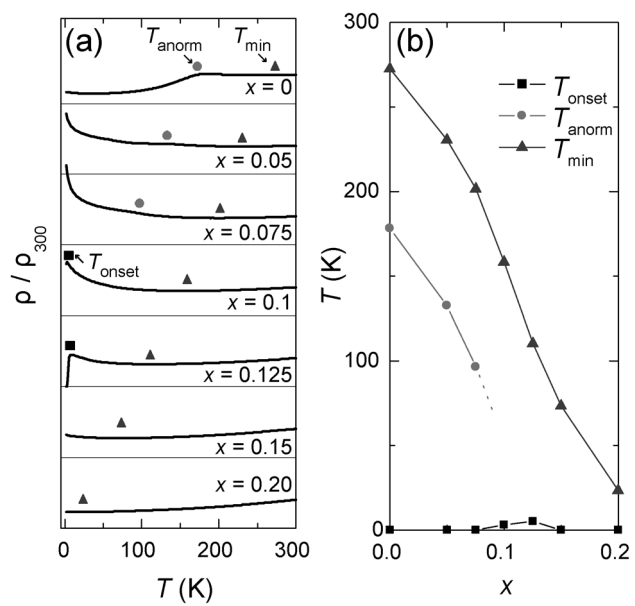


Fig. 3